Geoderma, 39 (1986) 105—123
Elsevier Science Publishers B.V., Amsterdam — Printed in The Netherlands

PROPERTIES OF IRON OXIDES IN SOME NEW CALEDONIAN OXISOLS

U. SCHWERTMANN and M. LATHAM*[1]

Lehrstuhl für Bodenkunde, Technische Universität München, D 8050 Freising 12 (F.R.G.)
O.R.S.T.O.M., 24 Rue Bayard, 75008 Paris (France)

(Received November 18, 1985; accepted after revision June 16, 1986)

ABSTRACT

Schwertmann, U. and Latham, M., 1986. Properties of iron oxides in some New Caledonian oxisols. Geoderma, 39: 105—123.

Oxisols from two toposequences of New Caledonia formed from peridotite, consist essentially of Fe oxides (goethite, hematite, maghemite). These Fe oxides were characterized by their mineralogy, crystal size and morphology, Al substitution, thermal behaviour and dissolution kinetics in 6 *M* HCl at 25° C.

In one toposequence the samples were free of hematite (goethite only) at > 1050 m above sea level whereas at lower altitudes hematite was also present. Al substitution was generally low due to the low Al content of the peridotite, except in gibbsitic samples on rocks somewhat higher in Al. The surface areas of goethite and hematite ranged between 50 and 150 $m^2 g^{-1}$. Dithionite-extractable Ni and Cr were between 0.2 and 2.2% Ni and 0.3 and 2.3% Cr. The hematite-containing samples tended to be higher in Cr and lower in Ni, whereas the opposite held for samples containing goethite only. Maghemites had a low unit cell size (8.31—8.32 instead of 8.34—8.35 Å) which was attributed to Al substitution. Dehydroxylation temperature of goethites was weakly correlated with Al substitution. Dissolution kinetics could be described by a linear form of a modified first-order reaction with one straight line for samples containing goethite only and two lines for samples containing goethite plus hematite.

INTRODUCTION

Highly weathered Oxisols (Acrorthox, sols ferrallitiques ferritiques) are formed under a wet tropical climate from ultrabasic rocks in New Caledonia. The extremely low Al content of the parent peridotite (dunite, harzburgite, lherzolite) and the complete removal of Si and Mg have led to an extraordinarily high concentration of residual Fe oxides in the bulk soil. In extensive studies of these soils, Latham (1975, 1985) found Fe concentrations up to 70—75% Fe_2O_3 with 3—8% Cr_2O_3, 3—15% Al_2O_3 and only

*[1]Present address: IBSRAM, P.O. Box 109, Bengklien, Bangkok 10900 (Thailand)

0016-7061/86/$03.50

0.5—1.7% SiO_2. Therefore, these soils offer a favourable possibility to characterize soil Fe-oxides without the need for any concentration procedures (such as boiling NaOH), which may or may not alter the properties of the Fe-oxides.

In one of the ultrabasic massifs studied — Boulinda, in the central part of the island, maximum altitude 1250 m — Latham (1975) noticed a change in the Fe oxide mineralogy as a function of altitude: whereas the soil at 1050 m and above, acid and rich in organic matter, contained only goethite, the soils at lower altitude contained both goethite and hematite. Additionally, crystallinity of the goethites was lower at the higher altitude.

On the other massif studied — Tiebaghi in the northwest part of the island with a maximum altitude of 600 m — goethite and hematite were nearly always associated. Also, gibbsite occurred in several samples as the parent material (lherzolite, harzburgite with clinopyroxene) was richer in aluminium (1—4%).

Geomorphologically, the massifs (Latham 1977, 1985) consist of five residual surfaces at various altitudes. This is believed to reflect differing climatic conditions during the uplift of the island. Both hot humid and subarid periods are assumed to have taken place between the late Tertiary and the present. Currently, the island has an average annual temperature of 23—24°C with a decrease of 0.5°C per 100 m increase in altitude and an average annual rainfall which increases from about 800 mm in the lowlands of the east coast up to 3000 mm in the highest part of the mountains. The distribution of the soils and their mineralogy appears to reflect both the climatic history of this area and the present climatic gradients caused by altitudinal differences.

This paper describes the iron oxides of the highly weathered and highly desilicified soils on the higher parts of these two peridotitic massifs.

MATERIALS AND METHODS

Samples from soils at various altitudes were taken during a field excursion in 1982. To complete the altitudinal series, a sample was also taken from a broken ferricrete in the coastal plain at about 8 m above the creek level at Moinda. Brief descriptions of the samples are given in Table I.

The samples were either analysed as such or crushed in a mortar if cemented. Where a magnetic phase was present, it was concentrated with the help of a hand magnet.

The following methods were used to characterize the Fe oxides chemically and mineralogically: Fe, Al, Cr and Ni extraction by dithionite-citrate-bicarbonate (Fe_d, Al_d, Cr_d, Ni_d), Fe by acid NH_4 oxalate (Fe_o, Schwertmann, 1964). Among the various dithionite methods the cold method was found to be more effective than the more common 85°C-method of Mehra and Jackson (1960). 10 mg of sample were extracted with 20 ml of the usual 0.3 *M* Na-citrate-$NaHCO_3$ mixture and 0.5 g of solid Na-dithionite

TABLE I

Description of samples

Sample no.	Geomorphic position	Horizon, depth (cm)	Description
Boulinda massif			
Bou 1	near summit of Mt. Boulinda at 1250 m, under tropical forest	just below C-rich Ah ca. 30	bright yellow clay, friable
Bou 2	as Bou 1, but at 1100 m	at soil surface	hollow, cylindrical root concretion
Bou 3	at ~ 1050 m	Ah; 0—20	bright yellow clay, friable
Bou 4	ditto	B; 40—50	ditto
Bou 5	ditto	at surface	dark brown crust, relic
Bou 5a	ditto	at surface	dark brown crust, newly formed
Bou 6	at ~ 800 m	B; 20—40	reddish clay with concretions
Bou 7	ditto	B; 40—60	reddish clay with concretions
Bou 8	ditto, different profile	B; 10—40	reddish clay with concretions
Bou 9	ditto	—	surface crust
Bou 10	at ~ 500 m	A; 0—20	purple clay, friable
Bou 11	at ~ 300 m	A; 0—20	concretionary layer, concretions
Bou 12	ditto	B; 30—40	red clay, friable
Tiebaghi massif			
Tib 1	at ~ 500 m, highest surface	—	crust, yellowish brown
Tib 2	ditto	—	crust, reddish brown
Tib 3	ditto	—	newly formed crust in doline
Tib 7	ditto	~ 15 m below surface	crust
Tib 5	at ~ 100 m	0—20	soil profile with reddish clay concretions and pieces of
Tib 6	ditto	20—40	crust
Coastal plain			
Moi 1		at surface	pieces of crust

for 16 h at room temperature (Holmgren, 1967). For complete dissolution of goethite and hematite by dithionote, particularly for cemented samples it was generally necessary to spex the samples (20 min). This shows that the resistance of goethite and hematite to complete reduction in dithionite, sometimes reported (Mendelovici et al., 1979), it is likely to be due to lack in fineness of the sample rather than to high crystallinity of the Fe oxides. This does not apply to maghemite which is rather resistant to reduction with dithionite (Taylor and Schwertmann, 1974). Gibbsitic samples were investigated untreated and also after boiling in 5 *M* NaOH to remove the gibbsite (Kämpf and Schwertmann, 1982).

Mineralogical analysis was carried out by X-ray diffraction using a Philips instrument with CoKα radiation and a diffracted beam monochromator. The hematite/goethite ratio was determined from the XRD peak intensity (peak height times peak width at half height) of the (012) line of hematite ($\times$ 3.5) and the (110) line of goethite. The relative proportions of accessory minerals (quartz, talc, gibbsite, chromite) were obtained from DCB-treated samples in which those minerals are effectively concentrated. The Al substitution of goethite was derived from the c-dimension of the unit cell (Schulze, 1984) using d(111) and d(110), accurately measured in relation to the nearby (012) and (104) lines of corundum (25%) admixed to the sample as an internal standard. Al substitution of goethite in samples containing goethite as the sole Fe-oxide was also calculated from Al_d and Fe_d. Al substitution of hematite was computed using the a-dimension of the unit cell as derived from d(300) and the relationship: Al = 678 (5.0418–a) obtained from Al hematites synthesized at 25°C. The unit cell size of maghemites was determined from the exact position of the (220), (311), (400), (511) and (440) lines using CaF_2 as an internal standard.

Crystallinity was characterized by the mean crystallite dimension (MCD), using the Scherrer formula. The widths at half height of certain strong XRD lines were corrected for instrumental broadening by using coarse crystalline quartz. For goethites, only MCD(110) and MCD(111) were calculated. For hematite, MCDa and MCDc (MCD in the crystallographic a- and c-directions) were taken from average MCD (hkl) values, namely from (110) and (300) for MCDa and from (021), (104), (110), (113) and (116) for MCDc (Schwertmann and Kämpf, 1985). DTA curves were run with 50—60 mg samples in the Pt crucible of a Linseis instrument under N_2 at a heating rate of 10°C min^{-1}. Surface area was measured by adsorption of ethylene-glycol-mono-ethylether (EGME; Carter et al., 1965). For samples containing only goethite or goethite and hematite, the surface area was also calculated from the specific surface of these two minerals and their contents in the sample. For this purpose the specific surface of goethite was taken from a relationship found between the corrected WHH(111) and the surface area S of 67 synthetic goethites: S (m^2 g^{-1}) = 202 · WHH(111) –4 (r = 0.955). Likewise, the specific surface area of hematite was calculated from its crystal dimensions MCDa and MCDc, assuming cylindrical crystals

and a density of 5.26 g cm^{-3}. The hematite- and goethite-contents of the samples were estimated from their ratios obtained from XRD (see Table III) and either Fe_d and Al substitution or weight loss after DCB treatment. Dissolution kinetics were studied using 6 *M* HCl at 25°C (Schwertmann, 1984a). TEM observations were carried out with a Zeiss EM 10 instrument.

RESULTS AND DISCUSSION

Mineralogical composition

As seen from XRD, all samples were essentially free of layer silicates except for talc in some samples. The absence of clay silicates is most likely due to the low Al content of the parent rocks and the complete removal of Mg and Si in the upper part of the weathering profile. By these processes, Fe was concentrated to such an extent that Fe oxides dominated all samples investigated.

Among the Fe oxides goethite and hematite prevail (Table II). This is in line with the generally low Fe_o/Fe_d values. At Boulinda, goethite is the sole Fe-oxide at an altitude of 1050 m and above, whereas below this altitude hematite is always present in addition to goethite. This fully agrees with the results of Latham (1975). Besides goethite and hematite, higher concentrations of maghemite are found in concretions of Bou 11 associated with a rather high Hm/(Hm+Gt) ratio of 0.72.

On Tiebaghi, goethite is always associated with some hematite, except in two crust samples. One of these was taken from a recent crust developed in a swampy doline where the absence of hematite may reflect the redox conditions. Some peat dated 30 000 years BP was found under this crust (Latham, 1985). The same applies to the sample taken in a hydromorphic soil in the coastal plain (Moi 1, Table II). Maghemite was found in magnetic nodules (2—5 mm size) of Tib 5 and 6 (Table II) again associated with rather high Hm/(Hm+Gt) ratios of 0.78 and 0.84 (Table III). The association of maghemite with an Hm/(Hm+Gt) ratio higher than in the surrounding soil (and its Al substitution, see below) was recently attributed to the effect of burning, leading to maghemite and hematite formation from goethite (Schwertmann and Fechter, 1984).

Besides Fe oxide minerals, chromite inherited from the parent rock is usually present in small amounts. It appears to be the most stable amongst the primary minerals, although evidence of dissolution appears on SEM photos (Latham, 1985). The unit size of the chromite was 8.17 Å in the Tiebaghi samples and 8.23 Å in the Boulinda samples, indicating some differences in composition. The chromite of Tiebaghi is richer in Al than that of Boulinda (Moutté, 1979; Latham, 1985) which is consistent with the results of Schellmann (1978).

Quartz is present in trace amounts in most samples. Its secondary formation under well-drained conditions was shown by Latham (1985). Talc

TABLE II

Physical, mineralogical and chemical properties

Sample	Colour dry	Subsample	Fe_d (%Fe)	Fe_o (%Fe)	$Fe_{o/d}$ ($\times 10^2$)	Ni_d (%Ni)	Cr_d (%Cr)	Mineralogy*[1]
Bou 1	7.5YR 5/8	fine earth	38.5	0.48	1.3	0.96	0.32	Gt > Qu > Ta
Bou 2	7.5YR 5/6	root concretion	50.2	0.55	1.1	0.87	0.64	Gt >> Qu > Ta
Bou 3	7.5YR 4/6	fine earth	48.7	0.47	1.0	2.16	0.34	Gt >> Qu > Chr, Ta
Bou 4	10YR 5/8	fine earth	43.2	0.69	1.6	1.43	0.84	Gt >> Ta > Qu > Chr
Bou 5	7.5YR 4/4	crust	48.3	0.33	0.7	0.59	1.49	Gt >> Qu > Chr
Bou 5a	7.5YR 5/6	crust	49.1	0.67	1.4	0.43	1.08	Gt >> Qu > Chr > Ta
Bou 6	5YR 4/6	fine earth	44.5	0.47	1.1	0.23	2.03	Gt >> Hm > Qu, Chr
Bou 7	7.5YR 5/8	fine earth	50.3	0.29	0.6	1.00	1.65	Gt >> Hm > Chr > Qu
Bou 8	2.5YR 3/4	fine earth	53.9	0.62	1.2	0.28	2.26	Hm > Gt > Mh > Chr > Qu
Bou 9	5YR 4/6	crust	47.3	0.34	0.7	0.45	2.23	Gt > Hm > Qu, Chr
Bou 10	2.5YR 3/6	20 μm	51.4	0.23	0.5	0.65	1.16	Gt > Hm >> Qu > Chr, Ta
Bou 10a	5YR 3/4	concretions	47.8	0.26	0.5	0.31	1.49	Gt > Hm > Chr, Mh, Qu
Bou 11	5YR 3/3	concretions	54.6	0.45	0.8	0.23	1.54	Mh > Hm > Gt > Chr > Qu
Bou 12	2.5YR 3/5	20 μm	47.8	0.15	0.3	0.50	1.38	Gt ~ Hm > Qu > Chr
Bou 12a	5YR 3/4	concretions	44.6	0.20	0.5	0.38	2.03	Hm > Gt > Mh, Qu, Chr
Moi 1		crust	38.4	0.37	1.0	0.13	0.56	Gt > Qu > Chr > Ta
Tib 1	5YR 4/8	crust	49.3	0.23	0.5	0.20	1.26	Gt >> Hm > Gb
Tib 2	2.5YR 3/6	crust	43.6	0.08	0.2	0.30	0.45	Hm > Gt > Gb > Chr
Tib 3	10YR 5/8	crust	22.8	0.06	0.3	0.36	1.73	Gt > Gb > Chr
Tib 5a	5YR 3/4	crust	49.0	0.36	0.9	0.37	1.21	Gt ~ Hm >> Qu, Chr
Tib 5b	5YR 4/5	fine earth	42.0	1.08	2.6	0.84	0.91	Gt > Hm >> Qu > Chr
Tib 5c	5YR 3/4	non-magnetic concretions	51.5	0.49	1.0	0.57	1.56	Hm ~ Gt >> Qu
Tib 5d	5YR 3/4	magnetic concretions	57.6	0.73	1.3	0.45	1.55	Mh > Hm > Gt >> Qu
Tib 6a	5YR 4/6	fine earth	44.4	0.29	0.7	0.94	0.86	Gt > Hm >> Qu > Chr
Tib 6b	5YR 4/5	non-magnetic concretions	50.4	0.59	1.2	0.56	1.77	Hm ~ Gt >> Qu
Tib 6c	5YR 3/4	magnetic concretions	58.1	0.72	1.2	0.39	1.48	Mh > Hm > Gt > Qu, Chr
Tib 7	5YR 5/7	crust	47.8	0.04	0.1	1.04	1.53	Gt > Hm > Gb

*[1] Gt: goethite; Hm: hematite; Mh: maghemite; Gb: gibbsite; Qu: quartz; Chr: chromite; Ta: talc.

TABLE III

Properties of goethites and hematites

Sample	Hm	Surf.area ($m^2 g^{-1}$)		Properties of goethites					Properties of hematites			
	(Hm+Gt)	EGME	calc.	MCD (110) (nm)	MCD (111) (nm)	Al-subst. XRD Al_d (mole %)		DTA end. (°C)	Surf.area WHH(111) ($m^2 g^{-1}$)	MCDa (nm)	MCDc (nm)	Al-subst. (mole %)	Surf.area MCDa, MCDc ($m^2 g^{-1}$)
Bou 1	0	129	65	14	16	1	3	255	121	—	—	—	—
Bou 2	0	102	56	24	26	6	5	278sh	73	—	—	—	—
Bou 3	0	169	55	20	25	3	3	260	76	—	—	—	—
Bou 4	0	213	63	17	20	6	8	260sh	98	—	—	—	—
Bou 5	0	79	43	30	33	9	12	286	57	—	—	—	—
Bou 5a	0	82	60			7		218	77	—	—	—	—
Bou 6	0.15	62	38	30	30	6	—	276	63	—	—	—	—
Bou 7	0.06	149	76	16	19	4	—	282	104	—	—	—	—
Bou 8	0.62	72	39	27	26	6	—	278	73	38	18	70	41
Bou 9	0.27	58	47	27	26	5	—	296	73	32	18	6	45
Bou 10	0.25	119	62	21	22	11	—	280	87	29	16	12	50
Bou 10a	0.53	50	48	25	23	12	—	297	83	31	14	12	52
Bou 11	0.72	—	—	18	n.d.	—	—	278	—	—	—		
Bou 12	0.43	98	54	23	25	13	—	288	76	26	12	14	61
Bou 12a	0.61	57	47	27	20	—	—	297	98	25	10		53
Tib 1	0.14	125	79	17	15	10	12	284	129	—	—	—	—
Tib 2	0.73	22	9	18	n.d.	8	—	277	—	95	32	8	20
Tib 3	0	96	34	25	25	20	23	328	78	—	—	—	—
Tib 5a	0.43	60	68	15	15	12	—	304	129	24	12	12	63
Tib 5b	0.36	78	62	18	16	7	—	291	121	21	10	10	74
Tib 5c	0.59	33	58	23	23	—	—	303	83	19	9	—	82
Tib 5d	0.78		27	18	—	—		275	—	22	14	—	62
Tib 6a	0.27	59	50	24	25	14	—	302	76	21	10	11	74
Tib 6b	0.55	114	60	23	22	13	13	302	87	16	12		79
Tib 6c	0.84	31	39	22	—		—	288	—	21	15		62
Tib 7	0.17	149	87	17	14	7	—	300	139	—	—	—	—
Moi 1	0	73	54	23	21	2	—	261	91	—	—	—	—

was also found in the deferrated residues. Gibbsite occurs only in the Tiebaghi samples from the highest surface.

Properties of iron oxides

(1) Mean crystallite dimension (MCD) and crystal morphology

The mean crystallite dimension (MCD) of goethites perpendicular to (110) and (111) lie between 14 and 33 nm (Table III). The frequency distribution of WHH(110) for 256 goethites from various soil environments peaked around 17 nm (Schwertmann, 1984b) indicating a somewhat higher crystallinity of the goethites in the Caledonian Oxisols, which is in agreement with data on those from Brazil (Schwertmann and Kämpf, 1985). A decrease in crystallinity with increasing altitude in the Boulinda sequence as suggested by Latham (1975) was not obvious from MCD values.

The crystal dimensions of hematites always show higher values for MCDa than for MCDc confirming the platy nature of the hematite crystals. Therefore, in this range, lines with $l \neq 0$ are usually broader than those with

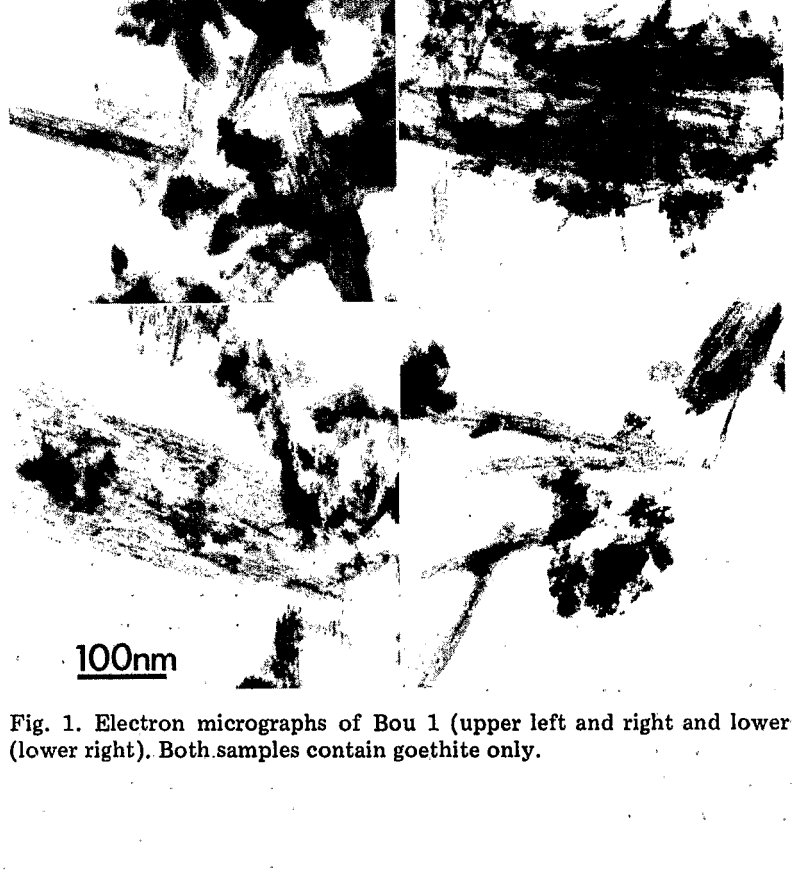

Fig. 1. Electron micrographs of Bou 1 (upper left and right and lower left) and Bou 3 (lower right). Both samples contain goethite only.

$l = 0$ (differential line broadening) as observed for hematites in soils from southern Brazil but also for synthetic hematite prepared at a low temperature (< 70°C) in the presence of Al. Al seems to retard growth in the c-direction (Schwertmann et al., 1979; Barron and Torrent, 1984).

Crystal size and morphology can also be deduced from *electron microscopy*. The goethite crystals in samples Bou 1 and 3 show pronounced acicularity (Fig. 1). The interior appears striated in the crystallographic c-direction which is not believed to be due to dehydration under the electron beam. On the other hand, it is equally unlikely that the crystals are in fact bundles of very thin needles. If this were the case, the needle width would be around 3—5 nm which would give an XRD width at half height (WHH) of 2—3° 2θ. The measured corrected WHH of the (020) line which directly reflects the width of the needle (MCDb) is only around 0.5° 2θ and corresponds to an average MCDb of about 15 nm, being more in line with the overall width of many of the crystals seen in Fig. 1. Therefore, what appear to be bundles of needles may in fact be coherently scattering crystals.

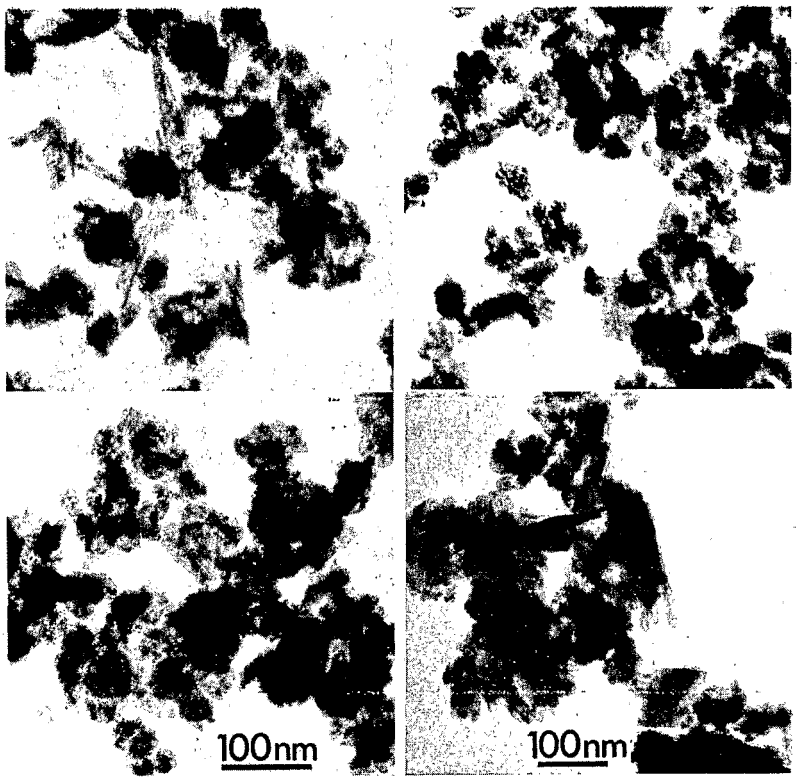

Fig. 2. Electron micrographs of Bou 5 (upper and lower left) containing goethite only and of Bou 8 (upper right) and Tib 2 (lower right) containing both goethite and hematite.

A similar goethite morphology appears in sample Bou 5 (Fig. 2) although much smaller, isodimensional goethite crystals can also be found. Isodimensional crystals prevail in the two samples containing hematite and goethite (Bou 8 and Tib 2). Isodimensional goethite and hematite crystals have been observed in other Oxisols (Kitagawa and Möller, 1979; Schwertmann and Kämpf, 1985; Schwertmann and Taylor, 1986). In such samples the morphological distinction of hematite from goethite is not possible.

SEM observations (Latham, 1985) have shown anisotropic goethans of acicular structure around voids whereas other parts of the s-matrix appear isotic. The isodimensional small goethite crystals may cause their rapid initial dissolution in HCl (see below).

(2) Al-substitution

The Al-substitution of the goethites studied ranged between 1 and 20 mole % with an average of 8 mole %. Considering an accuracy of ± 2 mole % for the XRD method (Schulze, 1984) the agreement between the values obtained from XRD (c-dimension) and from chemical analysis (Al_d) is surprisingly good, most probably because the samples do not contain any other Al compounds which could release Al into the CBD extract. The generally low substitution of the goethites as compared to Oxisols from other regions containing kaolinite and gibbsite (Schwertmann, 1984a, surely reflects the low Al content of the parent peridotite. In addition, Latham (1975) noticed an increase in the fulvic acid fraction with increasing altitude which may complex Al and thereby prevent its incorporation in the goethite structure.

A very low Al substitution was also found in the ferricrete on the lowest terrace, possibly reflecting an absolute Fe accumulation under hydromorphic conditions in the form of ferrans. Latham (1985) found by microprobe that ferrans were poorer in Al than the surrounding matrix where the goethite has accumulated relatively; Fitzpatrick and Schwertmann (1982) also noticed low Al substitution in goethites from hydromorphic environments.

Interestingly, the highest value of 20 mole % occurs in the gibbsitic sample Tib 3. Latham (1985) found an increasing Al-substitution in Tiebaghi soils as the amount of gibbsite increased. As shown by Didier et al. (1983), gibbsite should not be in thermodynamic equilibrium with goethite of high Al substitution (> 20 mole %).

Al substitution in hematites could only be measured from d(300) in samples having an (Hm/(Hm+Gt) ratio of > 0.25. Using a correlation between Al content and the a-dimension of pure synthetic hematites prepared at room temperature, a range of 6—14 mole- % Al was obtained. These values are significantly higher than those obtained from a curve for hematites prepared at 70°C (Schwertmann et al., 1979). The latter lead to values which are generally lower than in the goethite of the same sample in accord with a corresponding difference in maximum substitution of hematite (17%) and goethite (33%). Unfortunately, the Al-substitution of

hematites cannot be reliably estimated in these samples from Al_d for comparison because of other Fe-oxides (goethite, maghemite) present. Moreover, the internal magnetic field obtained from Mössbauer spectrometry cannot be used because it is influenced both by Al substitution and crystallinity (Murad and Schwertmann, 1983).

(3) Surface area

The EGME-surface of the bulk samples ranged between 30 and 213 $m^2 g^{-1}$. The contribution of compounds other than Fe-oxides to these values is probably small for two reasons. The weight loss after DCB treatment is usually well above 90% and the residues consist mainly of coarse-grained minerals (quartz, chromite, talc) as seen from sharp XRD lines. For example, the residue of Bou 1 had an EGME-surface of only 13 $m^2 g^{-1}$.

The surface areas calculated from the individual surface areas of goethite and hematite and their proportion in a sample (see Materials and Methods) are much lower than the EGME-surfaces of the bulk sample if the amounts of goethite and hematite are derived from Fe_d. Somewhat higher values were obtained if the goethite and hematite contents are derived from weight loss on DCB-treatment rather than from Fe_d, but the values are still lower than those obtained by EGME adsorption. This discrepancy is assumed to be due mainly to an underestimation of the calculated surfaces of goethite and hematite based on crystal size. From EM observations (Figs. 1, 2) the crystals look highly serrated so that frayed edges may also contribute to the EGME surface. This is probably not reflected to the same extent in the overall crystal size as determined from XRD line broadening.

Notwithstanding these limitations, the surface areas obtained for goethites and hematites lie in the same range as in other highly weathered soils (for a review, see Schwertmann, 1986).

The surface area of hematites (62—82 $m^2 g^{-1}$) is lower than that of goethites (57—139 $m^2 g^{-1}$). A similar range (34—75 $m^2 g^{-1}$) was found by the same procedure for hematites of Brazilian Ultisols and Oxisols (Schwertmann and Kämpf, 1985), whereas somewhat higher values (76—119 $m^2 g^{-1}$) were obtained by Pena and Torrent (1984) for 15 hematites in Mediterranean soils.

(4) Dehydroxylation temperature of goethite

The endotherms of goethite peaks lay between 255° and 336°C. This wide range can be partly explained by the variation in Al-substitution. A positive although not strong correlation was obtained: T_{DTA} (°C) = 259 + 3.16 Al (mole-%) (n = 22, r = 0.827) (Fig. 3). Synthetic Al goethites also show a positive correlation between dehydroxylation temperature and Al substitution but only within each series of preparations, whereas no correlation was obtained when Al goethites from various modes of preparation were considered together (Schulze and Schwertmann, 1984). Crystal size was found to be a second factor influencing dehydroxylation temperature. Crystallinity may therefore also explain part of the variation at the same Al substitution in the present samples.

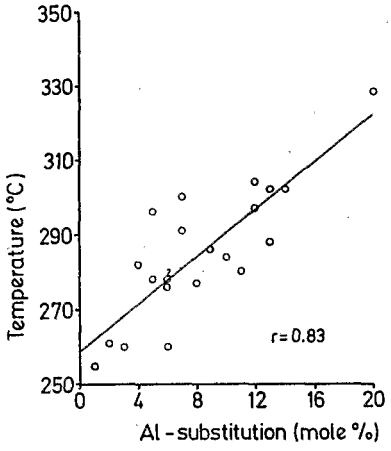

Fig. 3. Relation between Al substitution of goethites and dehydroxylation temperature with DTA.

Most of the dehydroxylation peaks are asymmetric and some have shoulders on the high temperature side. This is also the case for goethites from southern Brazilian soils (Kämpf, 1981, see also Schwertmann, 1984c) but also for synthetic Al goethites which often show a double peak (Schulze and Schwertmann, 1984). This behaviour was explained by a change in the unit cell size of the goethite before dehydroxylation to hematite takes place (Schwertmann, 1984c).

(5) Unit cell size of maghemites

A magnetic phase was concentrated from each of samples Bou 11, Tib 5 and Tib 6. The proportion of magnetic concretions in % of total concretions was 32 for Tib 5 and 18 for Tib 6.

The unit cell sizes of the maghemites in the three samples were 8.312(3), 8.323(4) and 8.323(5) Å for Bou 11, Tib 5 and Tib 6, respectively (the figure in parentheses gives the standard deviation of the last digit). These three figures are well below the value of 8.34—8.35 Å for pure maghemite and can be interpreted as due to substitution of Al for Fe in the cubic structure. By use of the calibration curve of Schwertmann and Fechter (1984) (a_o = 8.343 - 2.22 · 10^{-3} Al (mole-%); n = 28; r = 0.909) Al substitution for the 3 maghemites will be 14; 9 and 9 mole %. These are tentative values in view of the uncertainty of the experimental calibration curve.

(6) Nickel and chromium contents

The Ni-contents measured in the DCB extracts (Ni_d) ranged between 0.1 and 2%, a range found for nickeliferous laterites elsewhere in the world (see Schellmann, 1983). The highest values occurred in the Boulinda samples from the highest altitude, whereas the samples at lower altitudes, on Boulinda and Tiebaghi, and also samples from crusts are much lower in Ni_d.

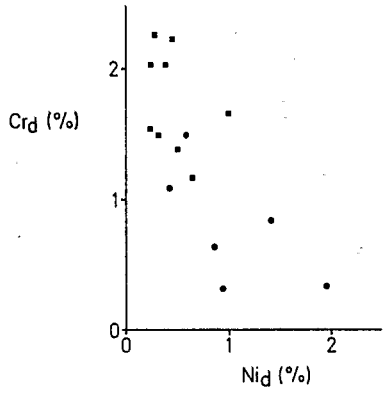

Fig. 4. Cr_d versus Ni_d in the Boulinda samples (• : samples with goethite only; ▪ : samples with hematite and goethite).

Lower values were also found in the young crust at the lowest altitude (Moi 1) and in two young crusts in older soils. All of these samples contain only goethite, and it is suggested that this "secondary" goethite has formed from primary goethite through a reduction-reoxidation process. It, therefore, would have had much less Ni available during its formation than the "primary" goethite formed immediately in the proximity of the Ni-supplying primary minerals of the peridotite.

Although the simultaneous extraction of Fe and Ni during the Fe oxide extraction by dithionite indicates association of Ni and Fe oxides it can not be considered as proof of Ni substitution for Fe in the goethite or hematite structure. Schellmann, through energy dispersive micro probe analysis (1983), dissolution kinetics (1978) and synthesis experiments (1980) (see also Kuxmann & Landau 1981) has produced some evidence for a possible substitution of Fe by Ni in goethite although definite structural proof is still lacking.

The values for Cr_d ranged between 0.2 and 2.0% Cr. Fig. 4 shows a plot of Cr_d versus Ni_d for the 13 Boulinda samples and a reciprocal relationship is obvious. There appears to be a trend for the samples containing goethite only to be high in Ni and low in Cr whereas the hematitic samples are low in Ni and high in Cr. This suggests that Cr may be concentrated more in (or on) hematite whereas Ni shows a higher affinity towards goethite. Cr-containing hematites have been synthesized at high temperature (1000°C) by a number of workers (see e.g., von Steinwehr 1967) and a complete solid solution between Fe_2O_3 and Cr_2O_3 was found.

Dissolution kinetics

Recent results with synthetic goethites have shown that Al substitution (Schwertmann, 1984a) and crystallinity (Schwertmann et al., 1985) affect dissolution kinetics in strong acids. The kinetic curves could not be de-

scribed by simple first-order kinetics. Kabai (1973) proposed the following modified first-order relationship which was successfully applied to sparingly soluble oxides and hydroxides:

$$C/C_0 = 1 - e^{-(kt)^{\alpha}} \quad (1)$$

where C and C_0 are the fractions dissolved at time t and $t = 0$, respectively, k is the rate constant and α is believed to be a phase-specific constant. A linear form of this equation is

$$\ln \ln 1/(1-C/C_0) = \ln K + \alpha \ln t \quad (2)$$

and a plot of the left-hand side of eq. 2 against ln t should yield a straight line. This was the case for a number of synthetic goethites (Schwertmann, 1984, Schwertmann et al., 1985) and also for goethites from soils (Schwertmann, 1986).

Dissolution curves for samples containing goethite only showed a single straight line (Fig. 5), whereas those containing goethite and hematite (Fig. 6) show two lines. The dissolution parameters k and α are summarized in Table IV. Samples from the two highest altitudes of the Boulinda sequences have a much higher dissolution-rate constant k than all the other goethites. This is in line with a lower crystallinity of those goethites as noticed by Latham (1975). For synthetic goethites of various crystallinities and Al substitution a k range of 0.1 - 30 · 10^{-3} min^{-1} was obtained, and k was predominately a function of the surface area and Al substitution (Schulze and Schwertmann, 1984; Schwertmann et al., 1985). As seen from Table IV most of the soil goethites lie in the lower part of the above k range indicating their high stability against proton attack. The goethite from sample Tib 3 showed an extremely low k value for the initial part of the dissolution and this sample had the highest Al substitution (20 mole %).

The physical meaning of α is not yet clear. Values of α for synthetic

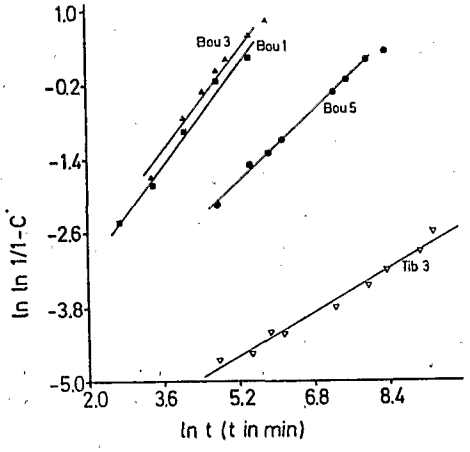

Fig. 5. Dissolution-time curves for goethitic samples (6 M HCl at 25° C).

TABLE IV

Dissolution parameters of selected samples (dissolution in 6 *M* HCl at RT)

Sample	Part	*n*	α	$k \cdot 10^3$ min.$^{-1}$	*r*	Hm/(Hm + Gt)	
						by XRD	by diss.
Bou 1	—	8	0.905	5.46	0.9917	0	0
Bou 3	—	7	1.104	8.60	0.9947	0	0
Bou 5	—	8	0.692	0.416	0.9977	0	0
Bou 8	I	5	0.589	0.450	0.9991	0.62	0.59
	II	3	0.442	0.421	0.9999		
Bou 10	I	4	0.983	0.68	0.9998	0.25	0.29
	II	4	0.706	0.44	0.9963		
Bou 12	I	4	1.184	0.68	0.9954	0.43	0.36
	II	4	0.643	0.375	0.9981		
Tib 2	I	4	2.11	1.78	0.9887	0.73	0.62
	II	5	0.457	1.69	0.9903		
Tib 3	—	9	0.443	0.00017	0.9902	0	0
Tib 5	I	4	0.824	0.440	0.9980	0.43	0.45
	II	3	0.505	0.297	0.9994		
Tib 7	I	3	1.927	0.470	0.9967	0.17	0.22
	II	4	1.045	0.255	0.9993		

goethites were between 1.3 and 1.8 and characterize an S-shape dissolution curve which was interpreted as an increase in surface area in the earlier part of the dissolution process. This received support from EM observations (Schwertmann, 1984a).

The values for the soil goethites, however, ranged between 0.4 and 2.1. A value of 1 corresponds to a first-order reaction whereas values < 1 and > 1 indicate an initial rate significantly higher or lower, respectively, than expected for a first order reaction.

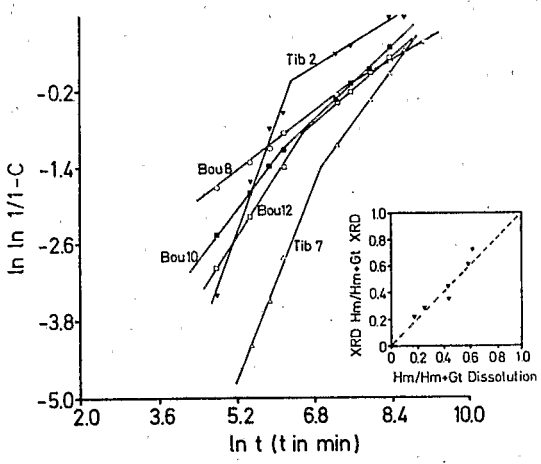

Fig. 6. Dissolution-time curves for goethitic-hematitic samples (6 *M* HCl at 25° C).

A split into two linear sections is evident for samples containing both goethite and hematite (Fig. 6). As shown by XRD the first part is due to hematite. Therefore, the proportion of hematite was calculated from the intersection of the two straight lines and compared with the goethite/hematite ratio as obtained from XRD. The insert in Fig. 6 shows that the two values agree reasonably well. Mixtures of goethite and hematite synthesized in the same system also show a much quicker dissolution of hematite than of goethite (Schwertmann, 1986). This dissolution method therefore offers a possibility for separating the two Fe oxides, although the separation effect may depend on the crystal morphology of the two oxides which differs among different soils (Figs. 1, 2).

CONCLUSIONS

The paper describes numerous properties of Fe oxides in Oxisols on ultrabasic rocks. Intense weathering under a moist tropical climate has led to a more or less complete exhaustion of the primary major elements of the rock except Fe, which was converted to Fe oxides. This has led to the formation of several meters of soil material with up to 50% Fe as Fe oxides. The oxides could therefore be studied in some detail without any concentration treatments.

The type of oxides was related to altitudinal changes in climate: hematite occurred in the lower (drier) parts of the mountains whereas the soils of the higher (moister) parts contain goethite only. Maghemite occurs only together with hematite. The quantification of goethite and hematite was done by XRD but dissolution-time curves (in 6 *M* HCl) were also able to separate these two oxides because hematite dissolved more quickly than goethite. The Al-for-Fe substitution in the oxide structure was generally low (< 10%) due to a low Al content of the parent rock. Al substitution was found earlier to reflect the pedoenvironment, and pH, Si concentration and degree of hydromorphism were among the controlling factors. This holds for rocks with ample supplies of Al, but the present study shows that Al-content of the rock can be an another factor. In Oxisols formed from rocks low in Al, hardly any clay silicates are formed, and thus Al-substitution in samples with goethite can also be estimated from Al_d (as shown by a good agreement with the Al substitution obtained from XRD). Al substitution in goethites appears to increase their dehydroxylation temperature. Maghemites had a smaller unit cell, which was also attributed to Al substitution.

The goethites consist either of elongated crystals 0.1—0.5 μm long with a striated internal structure — probably domains running parallel to the crystallographic c-direction — or of isodimensional particles some tens of nm in diameter. The latter morphology causes them to resemble hematite crystals so that they cannot be distinguished from them by their morphology.

The surface areas of the Fe oxides can only be determined with difficulties. Therefore, various methods were applied. The values obtained by direct determination with EGME suffer from impurities, and those calculated from XRD line broadening, i.e., from crystal dimensions, may not reflect the true surface. Nevertheless, the range found, namely 40—80 m^2 g^{-1} for hematites and 70—140 m^2 g^{-1} for goethites, agree with values found in other soils.

DCB extracts between 0.2 and 2.2% Ni and Cr. Because chromite, a common accessory mineral in these soils, does not dissolve in CBD, both metals must be associated with the Fe oxides. Ni appears to be more strongly associated with goethite, whereas Cr appears higher in the samples richer in hematite. The type of this association is not yet known.

A detailed study of the various properties of the iron oxides led us to conclude that the behaviour of these Oxisols is mainly governed by their iron oxides, firstly because of the high concentration of Fe oxides and secondly because of their minute crystal size and consequent high surface area. Iron oxide mineralogy and properties also provided information concerning the pedogenic environment.

ACKNOWLEDGEMENTS

The analytical help of Mrs. B. Gallitscher, U. Maul and Chr. Jud is gratefully acknowledged. Dr. H.-Ch. Bartscherev is thanked for the TEM photos. Dr. D.G. Lewis, University of South Australia, kindly revised the text. The senior author thanks the Deutsche Forschungsgemeinschaft for a travel grant.

REFERENCES

Barron, V. and Torrent, J., 1984. Influence of aluminum substitution on the color of synthetic hematites. Clays Clay Miner., 32: 157—158.

Carter, D.L., Heilman, M.D. and Gonzales, C.L., 1965. The ethylene glycol monoethyl ether (EGME) technique for determining soil-surface area. Soil Sci., 100: 409—413.

Didier, Ph., Nahon, D., Fritz, B. and Tardy, Y., 1983. Activity of water as a geochemical controlling factor in ferricretes. A thermodynamic model in the system: kaolinite Fe-Al-oxyhydroxides. In: D. Nahon and Y. Noack (Editors), Petrology of weathering and soils. Int. Colloq. CNRS, Paris: 35—44.

Fitzpatrick, R.W. and U. Schwertmann, 1982. Al-substituted goethite — an indicator of pedogenic and weathering environments in South Africa. Geoderma, 27: 335—347.

Holmgren, G.G.S., 1967. A rapid citrate-dithionite extractable iron procedure. Soil Sci. Soc. Am. Proc., 31: 210—211.

Kabai, J., 1973. Determination of specific activation energies of metal oxides and metal oxide hydrates by measurement of the rate of dissolution. Acta Chem. Acad. Sci. Hung., 78: 57—73.

Kämpf, N., 1981. Die Eisenoxidmineralogie einer Klimasequenz von Böden aus Eruptiva in Rio Grande do Sul, Brasilien. Dissertation, Technische Universität München, Germany, 271 pp.

Kämpf, N. and Schwertmann, U., 1982. Quantitative determination of goethite and hematite in kaolinitic soils by X-ray diffraction. Clay Miner., 17: 359—363.

Kitagawa, Y. and Möller, M.R.F., 1979. Comparative clay mineralogy of the 'Terra Roxa Estruturada' soil in the Amazon region. Soil. Sci. Plant Nutr., 25: 385—395.

Kuxmann, U. and Landau, M., 1981. Untersuchungen zur Typisierung von nickel-, kobalt- und chromführenden limonitischen Lateriterzen bei der schwefelsäuren Drucklaugung. Metall, 5: 408—417.

Latham, M., 1975. Les sols d'un massif de roches ultrabasiques de la Côte ouest de Nouvelle Caledonie, Le Boulinda, 2. Les sols à accumulation ferrugineuse relative. Cah. ORSTOM, Sér. Pedol., XIII: 159—172.

Latham, M., 1977. On geomorphology of northern and western New Caledonian ultramafic massifs. Int. Symp. Geodyn. South-West Pacif. Noumea (New Caledonia), Editions Technip, pp. 235—244.

Latham, M., 1985. Altération et pédogenèse sur roches ultrabasique en Nouvelle Caledonie. Genèse et évolution des accumulations de fer et de silice en relation avec la formation du modèle, Thèse d'état, Dijon, 331 pp. ORSTROM/(sous press).

Mehra, O.P. and Jackson, M.L., 1960. Iron-oxide removal from soils and clays by a dithionite-citrate system buffered with sodium bicarbonate. Clays Clay Miner., 7: 317—327.

Mendelovici, E., Yariv, S. and Villalba, R., 1979. Aluminiumbearing goethite in Venezuelan laterites. Clays Clay Miner., 27: 368—372.

Moutté, J., 1979. Le massif de Tibaghi (Nouvelle Caledonie) et ses gites de chromite. Thèse doct. Ing., ENSM, Paris, 156 pp.

Murad, E. and Schwertmann, U., 1983. The influence of aluminium substitution and crystallinity in the Mössbauer spectra of goethite. Clay Miner., 18: 301—312.

Pena, F. and Torrent, J., 1984. Relationships between phosphate sorption and iron oxides in Alfisols from a river terrace sequence of mediterranean Spain. Geoderma, 33: 283—296.

Schellmann, W., 1978. Behaviour of nickel, cobalt and chromium in ferruginous lateritic nickel ores. Bull. B.R.G.M., II, 3: 275—282.

Schellmann, W., 1980. Untersuchungen zur Typisierung und technologischen Verwertbarkeit Ni-, Co- und Cr-führender Lateriterze. Teil 2: Mineralogisch-geochemische Untersuchungen zur Konstitution und Bildung lateritischer Nickelsilikaterze. Abschlussbericht zum BMFT-Forschungsvorhaben R 001.

Schellmann, W., 1983. Geochemical principles of lateritic nickel ore formation. Proc. II Int. Seminar Laterisation Processes, Sao Paulo, 1982, pp. 119—135.

Schulze, D.G., 1984. The influence of aluminum on iron oxides. VIII. Unit-cell dimensions of Al-substituted goethites and estimation of Al from them. Clays Clay Miner., 32: 36—44.

Schulze, D.G. and Schwertmann, U., 1984. The influence of aluminium on iron oxides. X. The properties of Al-substituted goethites. Clay Miner., 19: 521—539.

Schwertmann, U., 1964. Differenzierung der Eisenoxide des Bodens durch photochemische Extraktion mit saurer Ammoniumoxalatlösung. Z. Pflanzenernähr., Düng., Bodenkd., 105: 194—202.

Schwertmann, U., 1984a. The influence of aluminium on iron oxides. IX. Dissolution of Al-goethites in 6 *M* HCl. Clay Miner., 19: 9—19.

Schwertmann, U., 1984b. The effect of pedogenic environments on iron oxide minerals. Adv. Soil Sci., 1: 172—200.

Schwertmann, U., 1984c. The double dehydroxylation peak of goethite. Thermochim. Acta, 78: 39—46.

Schwertmann, U., 1986. Some properties of soil and synthetic iron oxides. In: Iron in Soils and Clay Minerals. NATO-ASI, Bad Windsheim, GFR. In press.

Schwertmann, U. and Fechter, H., 1984. The influence of aluminium on iron oxides. XI. Aluminium-substituted maghemite in soils and its formation. Soil Sci. Soc. Am. J., 48: 1462—1463.

Schwertmann, U. and Kämpf, N., 1985. Properties of goethite and hematite in kaolinitic soils of southern and central Brazil. Soil Sci., 139: 344—350.

Schwertmann, U. and Taylor, R.M., 1986. Iron oxides. In: J.B. Dixon and S.B. Weed (Editors), Minerals in Soil Environments. Soil Sci. Soc. Am. J., Madison, Wisc., 2nd ed. In press.

Schwertmann, U., Cambier, Ph. and Murad, E., 1985. Properties of goethites with varying crystallinity. Clays Clay Miner., 33: 369—350.

Schwertmann, U., Fitzpatrick, R.W., Taylor, R.M. and Lewis, D.G., 1979. The influence of aluminum on iron oxides. Part II. Preparation and properties of Al-substituted hematites. Clays Clay Miner., 27: 105—112.

Steinwehr, H.E. v., 1967. Gitterkonstanten im System α-(Al, Fe, Cr)$_2$O$_3$ und ihr Abweichen von der Vergardregel. Z. Kristallogr. Mineral., 125: 377—403.

Taylor, R.M. and Schwertmann, U., 1974. Maghemite in soils and its origin, I. Properties and observations on soil maghemites. Clay Miner., 10: 289—298.